Template-free Hydrothermal Synthesis of CuO/Cu_2O Composite Hollow Microspheres

Huogen Yu,[†] Jiaguo Yu,*[,†] Shengwei Liu,[†] and Stephen Mann*[,‡]

State Key Laboratory of Advanced Technology for Material Synthesis and Processing, Wuhan University of Technology, Luoshi Road 122#, Wuhan 430070, P. R. China, and Centre for Organized Matter Chemistry, School of Chemistry, University of Bristol, Bristol, BS8 1TS, United Kingdom

Received February 7, 2007. Revised Manuscript Received June 22, 2007

CuO/Cu_2O composite hollow microspheres with controlled diameter and composition were prepared without the addition of templates and additives by hydrothermal synthesis using $Cu(CH_3COO)_2 \cdot H_2O$ as a precursor. Increasing the precursor concentration from 0.02 to 0.2 M increased the diameter of the composite hollow microspheres from 500 nm to 5 μm. Moreover, the content of Cu_2O in the composite hollow microspheres increased with increasing the reaction time or/and precursor concentration to produce a range of composite hollow microspheres with Cu_2O contents from 20 to 80 wt %. A localized Ostwald ripening mechanism was proposed to account for the formation of CuO/Cu_2O composite hollow microspheres. The photocatalytic activity experiment indicated that the prepared CuO/Cu_2O composite hollow microspheres exhibited a higher photocatalytic activity for the photocatalytic decolorization of methyl orange aqueous solution under the visible-light illumination than the single phase CuO or Cu_2O samples.

1. Introduction

Recently, inorganic hollow nanostructures with defined structure, composition, and tailored properties have attracted considerable attention because of their potentially numerous applications for the controlled release of various substances, catalysis, drug delivery, and protection of environmentally sensitive biological molecules and as lightweight filler materials and chemical reactors.[1−7] Among various synthesis methods, template-directed approaches have been demonstrated to be effective for preparing hollow microspheres. Various methods using hard templates (e.g., polymer latex, carbon, anodic aluminum oxide templates) or soft templates (e.g., supramolecular, ionic liquids, surfactant, organogel) have been extensively investigated.[8−13] These methods often involve the coating of nanocrystals on the template surface, followed by removal of the template using calcination or etching. The latter processes often compromise the structural integrity of the final product and so limit the application of the template-directed approach. In addition, using well-known physical phenomena such as the Kirdendall effect and Ostwald ripening, researchers have fabricated various hollow or porous nanostructures such as TiO_2, $SrTiO_3$, $BaTiO_3$. etc, in the absence of templates.[14−16] However, in general, it remains a major challenge to develop a facile, template-free, one-step solution route for the preparation of inorganic hollow nanostructures.

CuO and Cu_2O, p-type semiconductors with narrow band gaps (E_g (CuO) = 1.2 eV and E_g (Cu_2O) = 2 eV), have received much attention in recent years because of their various applications. CuO has been widely exploited for diverse applications as heterogeneous catalysts, gas sensors, superconductors, optical switches, lithium ion electrode materials, and field-emission emitters, whereas Cu_2O has been used in solar energy conversion, catalysis, electronics, and magnetic storage. In addition, CuO was demonstrated to have a complex magnetic phase, which formed the basis for several high T_c superconductors and materials with giant magnetoresistance. Considering their wide applications, various CuO and Cu_2O hollow nanostructures have been prepared.[17−20] Qi et al.[21] reported the one-pot synthesis of

* Corresponding author. E-mail: jiaguoyu@yahoo.com (J.Y.); s.mann@bristol.ac.uk (S.M.).
[†] Wuhan University of Technology.
[‡] University of Bristol.

(1) a) Caruso, F.; Caruso, R. A.; Mohwald, H. *Science* **199**8, *282*, 1111. (b) Caruso, F. *Chem.—Eur. J.* **200**0, *6*, 413. (c) Caruso, F. *Adv. Mater.* **200**1, *13*, 11. (d) Han, S.; Jang, B.; Kim, T.; Oh, S. M.; Hyeon, T. *Adv. Funct. Mater.* **2005**, *15*, 1845.
(2) Hu, J. S.; Guo, Y. G.; Liang, H. P.; Wan, L. J.; Bai, C. L.; Wang, Y. G. *J. Phys. Chem. B* **2004**, *108*, 9734.
(3) Xu, H.; Wang, W. Z.; Zhu, W.; Zhou, L. *Nanotechnology* **2006**, *17*, 3649.
(4) Xu, L.; Chen, X.; Wu, Y.; Chen, C.; Li, W.; Pan, W.; Wang, Y. *Nanotechnology* **2006**, *17*, 1501.
(5) Yao, B. D.; Chan, Y. F.; Zhang, X. Y.; Zhang, W. F.; Yang, Z. Y.; Wang, N. *Appl. Phys. Lett.* **2003**, *82*, 281.
(6) Sander, M. S.; Cote, M. J.; Gu, W.; Kile, B. M.; Tripp, C. P. *Adv. Mater.* **2004**, *16*, 2052.
(7) Yu, J.; Yu, H.; Cheng, B.; Trapalis, C. *J. Mol. Catal. A* **2006**, *249*, 135.
(8) Sun, Y.; Xia, Y. *Science* **2002**, *298*, 2176.
(9) Sun, X.; Liu, J.; Li, Y. *Chem.—Eur. J.* **2006**, *12*, 2039.
(10) Hoyer, P. *Langmuir* **1996**, *12*, 1411.
(11) Kobayashi, S.; Hanabusa, K.; Hamasaki, N.; Kimura, M.; Shirai, H. *Chem. Mater.* **2000**, *12*, 1523.
(12) Nakashima, T.; Kimizuka, N. *J. Am. Chem. Soc.* **2003**, *125*, 6386.
(13) Jung, J. H.; Kobayashi, H.; van Bommel, K. J. C.; Shinkai, S.; Shimizu, T. *Chem. Mater.* **2002**, *14*, 1445.
(14) Yang, H. G.; Zeng, H. C. *J. Phys. Chem. B* **2004**, *108*, 3492.
(15) Wang, Y.; Xu, H.; Wang, X.; Zhang, X.; Jia, H.; Zhang, L.; Qiu, J. *J. Phys. Chem. B* **2006**, *110*, 13835.
(16) Yin, Y. D.; Rioux, R. M.; Erdonmez, C. K.; Hughes, S.; Somorjai, G. A.; Alivisatos, A. P. *Science* **2004**, *304*, 711.
(17) Lu, C.; Qi, L.; Yang, J.; Zhang, D.; Wu, N.; Ma, J. *J. Phys. Chem. B* **2004**, *108*. 17825.

10.1021/cm070386d CCC: $37.00
Published on Web 07/28/2007

octahedral Cu_2O nanocages via a catalytic solution route. Zeng et al.[22,23] reported the preparation of hollow Cu_2O nanospheres from a reductive conversion of aggregated CuO nanocrystallites and the formation of CuO microspheres by a two-tiered organizing scheme. However, CuO/Cu_2O composite hollow nanostructures and their photocatalytic activity were seldom reported in these previous studies.

In this paper, CuO/Cu_2O composite hollow microspheres were prepared in the absence of templates and additives by a simple hydrothermal method using $Cu(CH_3COO)_2 \cdot H_2O$ as precursor. The CuO/Cu_2O composite hollow microspheres with a controllable diameter (500 nm to 5 μm) and composition (23.4−80.6 wt % Cu_2O) could be easily obtained by adjusting the precursor concentration and reaction time. A formation mechanism was proposed to account for the production of CuO/Cu_2O composite hollow microspheres. The photocatalytic activity of the samples was evaluated by the photocatalytic decolorization of methyl orange aqueous solution under the visible-light illumination in the presence of H_2O_2. To the best of our knowledge, this is the first report on the preparation and photocatalytic activity of CuO/Cu_2O composite hollow microspheres with a controllable diameter and composition by a template-free hydrothermal method. This work may provide new insights into preparing other inorganic hollow microspheres.

2. Experimental Section

2.1. Preparation. $Cu(CH_3COO)_2 \cdot H_2O$ was used as precursor for the preparation of CuO/Cu_2O composite hollow microspheres. In a typical synthesis, $Cu(CH_3COO)_2 \cdot H_2O$ powder was dissolved in distilled water to prepare the precursor solution with a concentration range of 0.02−0.2 M. Next, 35 mL of the precursor solution was transferred into a 50 mL Teflon-lined stainless steel autoclave, followed by a hydrothermal treatment at 200 °C for 1−36 h. After the reaction, the powder samples were filtered, rinsed with distilled water, and dried in a vacuum oven at 60 °C for 8 h.

2.2. Characterization. Morphology observations were performed on a JSM-5610LV scanning electron microscope (SEM, JEOL, Japan). X-ray diffraction (XRD) patterns were obtained on a D/MAX-RB X-ray diffractometer (Rigaku, Japan) using Cu Kα irradiation at a scan rate (2θ) of 0.05° s^{-1} and were used to determine the phase structures and the average crystallite size of the obtained samples. The accelerating voltage and applied current were 15 kV and 20 mA, respectively. Transmission electron microscopy (TEM) analyses were conducted with a JEOL 1200 EX at 120 kV. Nitrogen adsorption−desorption isotherms were obtained on an ASAP 2020 (Micromeritics Instruments, USA) nitrogen adsorption apparatus. The sample was degassed at 60 °C prior to BET measurements. The Brunauer−Emmett−Teller (BET) specific surface area (S_{BET}) was determined by a multipoint BET method using the adsorption data in the relative pressure (P/P_0) range of 0.05−0.25. Desorption isotherm was used to determine the pore size distribution using the Barret−Joyner−Halender (BJH) method.[24] The nitrogen adsorption volume at the relative pressure (P/P_0) of 0.994 was used to determine the pore volume and the average pore size.

2.3. Measurement of Photocatalytic Activity. The evaluation of photocatalytic activity of the as-prepared samples for the photocatalytic decolorization of methyl orange aqueous solution was performed at ambient temperature (ca. 24 °C). Experiments were as follows: 0.2 g of the prepared powders were dispersed in a 20 mL of methyl orange aqueous solution with a concentration of 3.1×10^{-5} mol L^{-1} in a dish (with a diameter of ca. 7.0 cm), followed by the addition of 0.1 mL of hydrogen peroxide solution (H_2O_2, 30 wt %). An 18-W daylight lamp (3 cm above the dish) was used as a light source. The integrated daylight intensity was 0.46 ± 0.01 mW/cm^2, as measured by a UV radiometer (made in the photoelectric instrument factory of Beijing Normal University) with the peak intensity of 420 nm. After the addition of H_2O_2, the mixed solution of catalysts and methyl orange was kept for 30 min, which allows the reaction system to reach adsorption equilibrium. The concentration of methyl orange aqueous solution was determined by a UV−visible spectrophotometer (UV-2550, SHIMADZU, Japan). After visible-light irradiation for 60 min, the reaction solution was filtrated, and the absorbance of methyl orange aqueous solution was then measured.

3. Results and Discussion

Figure 1a shows SEM image of the product obtained in a 0.1 M $Cu(CH_3COO)_2 \cdot H_2O$ aqueous solution treated at 200 °C for 12 h and reveals that the sample is in the form of hollow microspheres with a diameter of 1−2.5 μm. High-magnification SEM image (Figure 1b) displays that the shell wall of the hollow microspheres is composed of nanoparticles with a diameter of ca. 50 nm. The corresponding XRD results indicate the presence of two CuO and Cu_2O phases in the prepared hollow microspheres (see below in Figure 4c). Nitrogen adsorption−desorption isotherms were measured to determine the specific surface area and pore volume of CuO/Cu_2O composite hollow microspheres, and the corresponding results are presented in Figure 2. At a high relative pressure range between 0.4 and 1.0, the sample exhibites a type H3 hysteresis loop according to BDDT classification,[24] indicating the presence of slitlike mesopores (2−50 nm) in the CuO/Cu_2O composite hollow microspheres. The pore size distribution of composite hollow microspheres (Figure 2, inset) suggests a narrow pore size range from 2 to 15 nm with a maximum pore diameter of 3.4 nm. The S_{BET} and pore volume of hollow composite microspheres are 17.1 m^2/g and 0.04 cm^3/g, respectively. Considering the morphology of CuO/Cu_2O composite hollow microspheres (images a and

(18) Liu, Y.; Chu, Y.; Li, M.; Li, L.; Dong, L. *J. Mater. Chem.* **2006**, *16*, 192.
(19) Wang, D.; Mo, M.; Yu, D.; Xu, L.; Li, F.; Qian, Y. *Cryst. Growth Des.* **2003**, *3*, 717.
(20) Zheng, X. G.; Xu, C. N.; Tomokiyo, Y.; Tanaka, E.; Yamada, H.; Soejima, Y. *Phys. Rev. Lett.* **2000**, *85*, 5170.
(21) Lu, C.; Qi, L.; Yang, J.; Wang, X.; Zhang, D.; Xie, J.; Ma, J. *Adv. Mater.* **2005**, *17*, 2562.
(22) Chang, Y.; Teo, J.; Zeng, H. C. *Langmuir* **2005**, *21*, 1074.
(23) Liu, B.; Zeng, H. C. *J. Am. Chem. Soc.* **2004**, *126*, 8124.
(24) (a) Sing, K. S. W.; Everett, D. H.; Haul, R. A. W.; Moscou, L.; Pierotti, R. A.; Rouquerol, J.; Siemieniewska, T. *Pure Appl. Chem.* **1985**, *57*, 603. (b) Yu, J.; Liu, S.; Yu, H. *J. Catal.* **2007**, *249*, 59.

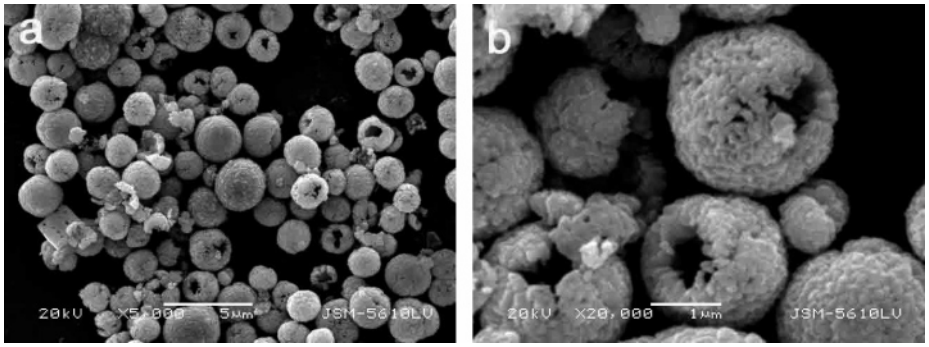

Figure 1. SEM images of CuO/Cu_2O composite hollow microspheres obtained in a 0.1 M $Cu(CH_3COO)_2 \cdot H_2O$ aqueous solution at 200 °C for 12 h.

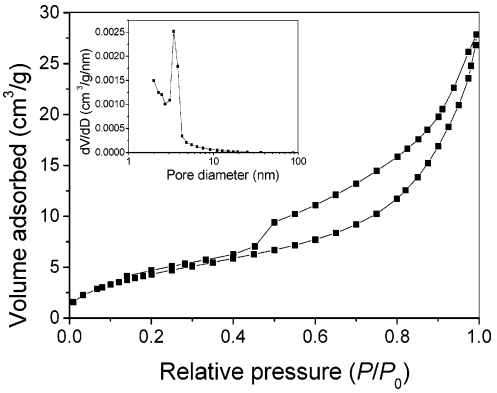

Figure 2. Nitrogen adsorption−desorption isotherm and corresponding pore size distributions (inset) of CuO/Cu_2O composite hollow microspheres obtained in a 0.1 M $Cu(CH_3COO)_2 \cdot H_2O$ aqueous solution at 200 °C for 12 h.

b of Figure 1), the formation of mesoporous structures (2−15 nm) is attributed to the aggregation of the nanoparticles within the shell wall of an individual hollow microsphere.

To investigate the formation mechanism of hollow composite microspheres, we studied the effect of reaction time on the morphology of products. Figure 3a shows the SEM image of the sample obtained in a 0.1 M $Cu(CH_3COO)_2 \cdot H_2O$ aqueous solution at 200 °C for 1 h. It can be seen that the obtained products are spherical particles with a diameter of 1−2 μm. The corresponding XRD pattern (Figure 4a) indicates that these spherical particles are pure CuO (space group $C2/c$; $a_0 = 4.683$ Å, $b_0 = 3.422$ Å, $c_0 = 5.128$ Å, $\beta = 99.54°$; JCPDS 72-0629). After reaction for 5 h, the morphology of the spherical particles (Figure 3b) has no obvious change. However, the XRD result (Figure 4b) indicates that the diffraction peaks of Cu_2O (space group $Pn3m$; $a_0 = 4.252$ Å; JCPDS 74-1230) are found in addition to the sharp diffraction peaks of CuO, indicating the formation of Cu_2O in these spherical particles. With increasing reaction time to 12 h, the individual microsphere becomes hollow and the shell wall consists of nanoparticles with a diameter of ca. 50 nm (Figure 3c). Moreover, the intensities of the diffraction peaks of CuO and Cu_2O increase significantly (Figure 4c). This is due to enhancement of crystallization of the composite hollow microspheres. With a further increase in the reaction time to 36 h, the size of nanoparticles in the shell wall of the individual microsphere increases to 150−300 nm. Further observations indicate that the hollow microspheres usually exhibit a single-layer structure of nanoparticles, resulting in the formation of macrospores (>50 nm) on the surface of hollow microspheres (Figure 3d). XRD pattern (Figure 4d) shows that the intensities of diffraction peaks of CuO decrease, whereas that of Cu_2O has an obvious increase. It can be deduced that CuO phase is gradually transformed into Cu_2O phase.

To characterize the growth of CuO and Cu_2O with increasing reaction time, the average crystallite sizes of CuO and Cu_2O in the composite products are calculated using Scherrer's equation for the main diffraction peaks of CuO (111) and Cu_2O (111) planes and the corresponding results are shown in Table 1. It can be seen from Table 1 that after hydrothermal treatment for 1 h, the crystallite sizes of the CuO is ca. 6.6 nm. Obviously, the spherical particles in Figure 3a are the aggregates of CuO nanocrystallites. With increasing reaction time to 36 h, the crystallite sizes of CuO increase gradually to 16.7 nm. The Cu_2O phase starts to appear after reaction for 5 h and the average crystallite size is 35.8 nm. With increasing the reaction time to 36 h, the average crystallite size of Cu_2O further increases to 45.7 nm.

Because there was no special reducing agent added in our reaction solution, it could be deduced that the CH_3COOH generated from the hydrolysis of $Cu(CH_3COO)_2$ had an obvious reducing action for the phase transformation of CuO to Cu_2O. The following reactions may occur

$$Cu(CH_3COO)_2 + 2H_2O \rightarrow Cu(OH)_{2\,(s)} + 2CH_3COOH \quad (1)$$

$$Cu(OH)_{2\,(s)} \rightarrow CuO_{(s)} + H_2O \quad (2)$$

$$8CuO_{(s)} + CH_3COOH \rightarrow 4Cu_2O_{(s)} + 2H_2O + 2CO_2 \quad (3)$$

The formation of solid-phase $Cu(OH)_2$ in reaction 1 was confirmed during the hydrothermal treatment process. XRD results (not shown here) indicated that blue $Cu(OH)_2$ powders were obtained when a 0.1 M $Cu(CH_3COO)_2$ aqueous solution was heated to 200 °C and then cooled to room temperature rapidly. In addition, the $Cu(OH)_2$ powder was easily dehydrated in water when the temperature was higher than 70 °C.[17] Therefore, CuO powder in reaction 2 could be obtained during further hydrothermal treatment. Similar to previous reports[22] that formic acid (HCOOH) acted as a weak reducing agent for the phase transformation of CuO to Cu_2O, in this study, CH_3COOH in reaction 3 resulted in the formation of CuO/Cu_2O composite hollow microspheres. To further confirm that CuO can be reduced by CH_3COOH, we added 2 mL CH_3COOH to a 35 mL distilled water containing 0.3 g of CuO powders, followed by the hydrothermal reaction

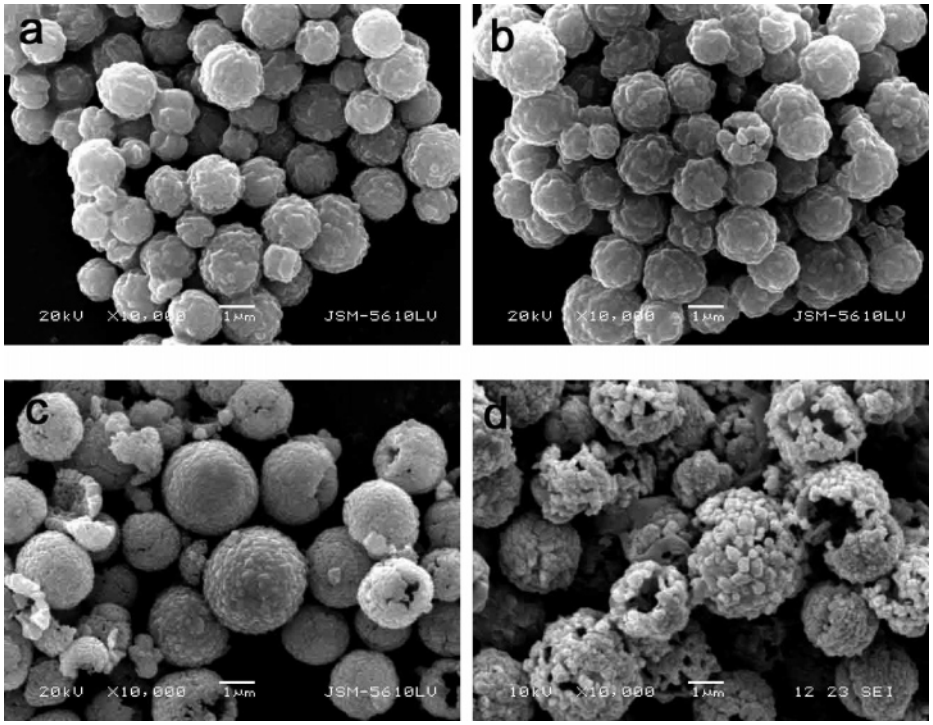

Figure 3. SEM images of CuO/Cu_2O composite hollow microspheres obtained in a 0.1 M $Cu(CH_3COO)_2 \cdot H_2O$ aqueous solution at 200 °C for (a) 1, (b) 5, (c) 12, and (d) 36 h.

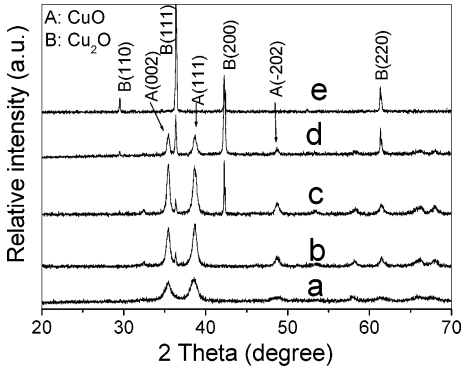

Figure 4. XRD patterns of CuO/Cu_2O composite hollow microspheres obtained in a 0.1 M $Cu(CH_3COO)_2 \cdot H_2O$ aqueous solution at 200 °C for (a) 1, (b) 5, (c) 12, (d) 36, and (e) 12 h (with the addition of 1 mL of CH_3COOH).

Table 1. Effects of Reaction Time and Precursor Concentration on the Phase Composition, Crystallite Size, Specific Surface Area, and Pore Volume

samples	W_{CuO} (%)	W_{Cu_2O} (%)	D_{CuO} (nm)	D_{Cu_2O} (nm)	S_{BET} (m^2/g)	$V_{pore\ volume}$ (cm^3/g)
1 h $_{(0.1\ M)}$	100	0	6.6	0	45.5	0.045
5 h $_{(0.1\ M)}$	79.9	20.1	10.5	35.8	23.1	0.041
12 h $_{(0.1\ M)}$	76.6	23.4	13.8	37.6	17.7	0.036
36 h $_{(0.1\ M)}$	31.8	68.2	16.7	45.7	4.7	0.008
5 h $_{(0.2\ M)}$	25.5	74.5	15.5	51.3	18.6	0.043
12 h $_{(0.2\ M)}$	19.4	80.6	17.7	66.9	4.0	0.014
24 h $_{(0.2\ M)}$	0	100	0	>100	0.3	0.002

at 200 °C for 12 h. It was found that after hydrothermal treatment, the color of the product changed from black into red. The corresponding XRD result (no shown here) showed that there were not the diffraction peaks of CuO phase in addition to the sharp peaks of Cu_2O phase, suggesting that the CH_3COOH in reaction 3 was a reducing agent for the formation of Cu_2O phase. Moreover, when 1 mL of CH_3COOH was added into a 35 mL $Cu(CH_3COOH)_2 \cdot H_2O$ aqueous solution (0.1 M) and the hydrothermal reaction was carried out at 200 °C for 12 h, only Cu_2O phase was formed (Figure 4e). This suggested that more CH_3COOH in the reaction system could accelerate the phase transformation rate of CuO to Cu_2O, resulting in the disappearance of the CuO phase after reaction for 12 h.

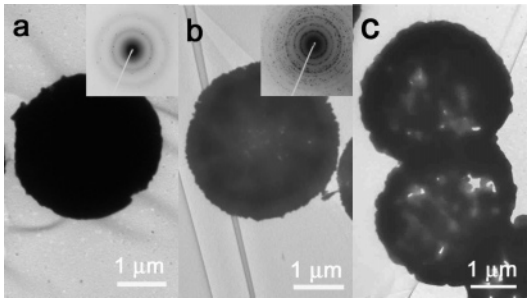

Figure 5. TEM images of CuO/Cu_2O composite hollow microspheres obtained in a 0.1 M $Cu(CH_3COO)_2 \cdot H_2O$ aqueous solution at 200 °C for (a) 1, (b) 12, and (c) 36 h.

According to previous studies,[25] the height of the characteristic diffraction peaks of CuO (111) and Cu_2O (111) planes can be used for calculation of the relative content of Cu_2O phase (wt %) in the CuO/Cu_2O composite hollow microspheres. The relative content of Cu_2O in the composite hollow microspheres is obtained according to the relative ratio $I_{Cu2O\ (111)}/(I_{CuO\ (111)} + I_{Cu2O\ (111)})$ and the calculated results are shown in Table 1. It can be observed from Table 1 that the relative content of Cu_2O increases from 20.1 to 68.2 wt % with increasing reaction time from 5 to 36 h when the 0.1 M $Cu(CH_3COO)_2 \cdot H_2O$ is used as the reaction solution. However, at 1 h, only pure CuO spherical particles were obtained. Therefore, it can be concluded that the CuO/Cu_2O

(25) Katsifaras, A.; Spanos, N. *J. Cryst. Growth* **1999**, *204*, 183.

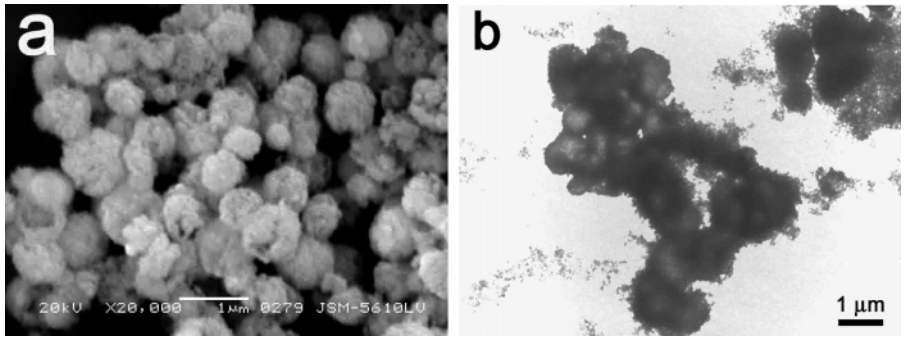

Figure 6. (a) SEM and (b) TEM images of CuO/Cu_2O composite hollow microspheres obtained in a 0.02 M $Cu(CH_3COO)_2 \cdot H_2O$ aqueous solution at 200 °C for 12 h.

composite solid microspheres with a controlled composition (Cu_2O wt% = 0−20.1 wt %) can be prepared by this hydrothermal method and may also provide a facile route for fabricating CuO/Cu_2O composite solid microspheres with a controllable composition.

The formation mechanism of CuO/Cu_2O composite hollow microspheres can be explained by a self-transformation process of the metastable aggregated particles accompanied by the localized Ostwald ripening.[26,27] Similar mechanisms have been used to prepare TiO_2, CuO, SnO_2, Fe_2O_3, $CdMoO_4$, and $ZnWO_4$ hollow spheres.[14,22,28] For the initial formation of aggregated precursor particles (Figure 3a), the CuO microspheres showed low diffraction peaks due to the presence of amorphous or poor crystallized phase (Figure 4a). This could be further confirmed by the broad diffraction rings in the electron diffraction analysis (Figure 5a, inset). TEM image indicated that these spherical particles were solid and no hollow structure was found (Figure 5a). In this stage, these aggregated CuO microspheres are not in thermodynamically equilibrium status and become metastable because of their large surface energy. Although the formation of amorphous or small crystallites is kinetically favored during the initial agglomeration, larger crystallites are thermodynamically favored.[26] To reduce the total surface energy, the formed metastable CuO nanoparticles (including the amorphous or poor crystallized particles and the crystalline particles with a diameter lower than critical size) would remain out of equilibrium with the surrounding solution because of their higher solubility, and so the core dissolves because of the existence of a diffusion pathway through the outer mesoporous crystalline shell. As a consequence, the supersaturation increases in the solution and then will be over the solubility of the crystalline CuO; secondary nucleation of CuO occurs on the external surface. Thus, the thickness of the crystalline shell increases as the amorphous core becomes progressively depleted to produce intact hollow microspheres. Figure 3 shows that with increasing reaction time from 1 to 12 h, the average diameter of the CuO microspheres increases and their surface becomes rough. The corresponding TEM image (Figure 5b) suggested the formation of hollow structure in the composite spherical particles, and the narrow diffraction rings of the samples (inset) indicated the enhancement of crystallization. Therefore, we believed that the metastable CuO nanoparticles in the interior were dissolved gradually and the new CuO nuclei were formed on the surface of the aggregated CuO microspheres within 12 h by a dissolution−crystallization mechanism.[26] This self-transformation process within the same aggregated particles was associated with localized Ostwald ripening mechanism, resulting in the obvious growth of the CuO nanocrystallites from 6.6 to 13.8 nm (Table 1) and the formation of hollow interior structure. With further increase in the reaction time to 36 h, this progressive redistribution of matter from the interior to the exterior of the microspheres controlled by a localized Ostwald ripening, resulted in the further increase in the crystallite size (Table 1) and the decrease in the electron density of the interior of the composite hollow microspheres (Figure 5c).

The above results highlight a facile hydrothermal route to the formation of CuO/Cu_2O composite hollow microspheres. The XRD results, along with those from SEM and TEM analysis, suggested that the formation of the composite hollow microspheres comprised as least three levels of structural organization: (1) aggregation of CuO nanoparticles containing amorphous or poorly crystallized phase to produce the metastable aggregated spherical particles; (2) redistribution and reassembly of CuO nanoparticles from the interior to the exterior of the microspheres to produce mesoporous hollow particles within 12 h; (3) phase transformation of CuO to Cu_2O in the presence of CH_3COOH during the hydrothermal treatment, resulting in the formation of CuO/Cu_2O composite structures. The diameter of the interior of hollow composite microspheres was determined by the size of as-formed aggregated solid particles. However, the absolute size of the aggregated solid particles may be mainly determined by the size and the aggregation tendencies of the primary particles, which were influenced by the experimental conditions such as concentration of precursor.[29]

The CuO/Cu_2O composite hollow microspheres with a smaller or larger diameter could be easily fabricated only by decreasing or increasing the precursor concentration of

(26) Yu, J. G.; Guo, H. T.; Davis, S. A.; Mann, S. *Adv. Funct. Mater.* **2006**, *16*, 2035.
(27) Colfen, H.; Mann, S. *Angew. Chem., Int. Ed.* **2003**, *42*, 2350.
(28) (a) Lou, X. W.; Wang, Y.; Yuan, C.; Lee, J. Y.; Archer, A. *Adv. Mater.* **2006**, *18*, 2325. (b) Yu, D.; Sun, X.; Zou, J.; Wang, Z.; Wang, F.; Tang, K. *J. Phys. Chem. B* **2006**, *110*, 21667. (c) Wang, W. S.; Zhen, L.; Xu, C. Y.; Zhang, B. Y.; Shao, W. Z. *J. Phys. Chem. B* **2006**, *110*, 23154. (d) Huang, J. H.; Gao, L. *J. Am. Ceram. Soc.* **2006**, *89*, 3877.
(29) Bogush, G. H.; Zukoshi, C. F. *J. Colloid Interface Sci.* **1991**, *142*, 1.

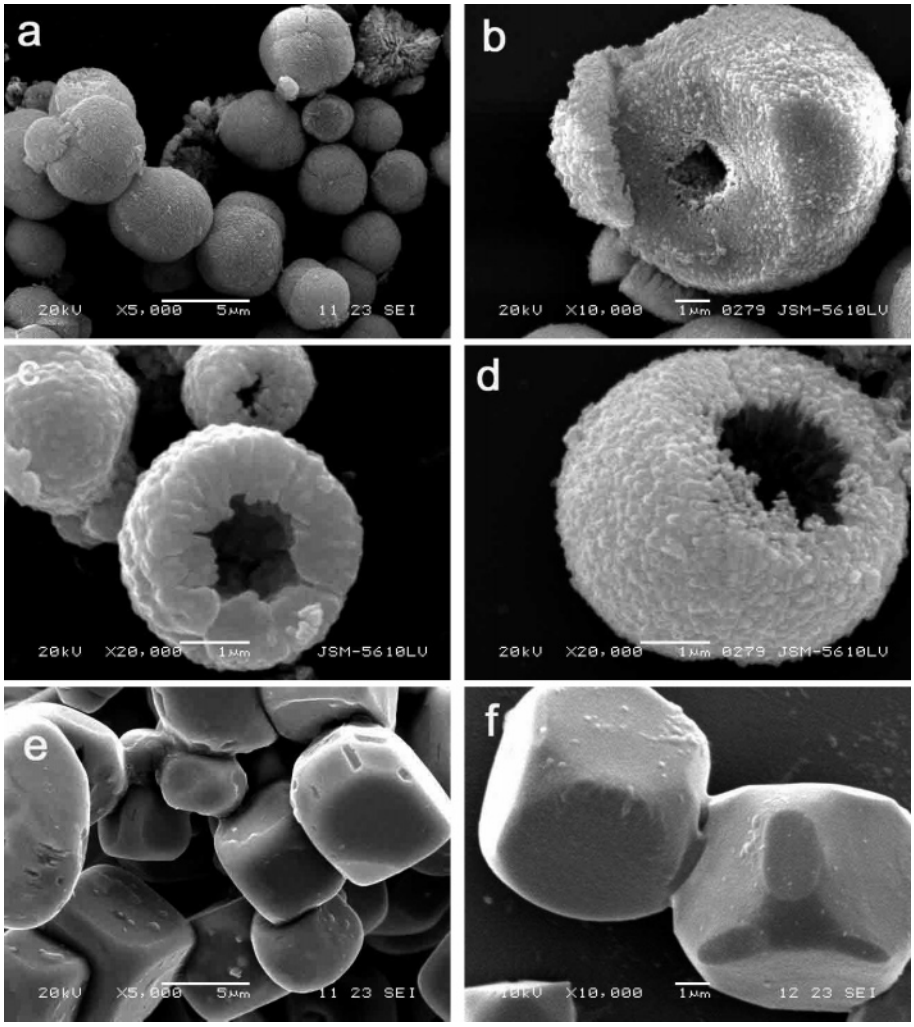

Figure 7. SEM images of CuO/Cu_2O composite hollow microspheres obtained in a 0.2 M $Cu(CH_3COO)_2 \cdot H_2O$ aqueous solution at 200 °C for (a, b) 5, (c) 8, (d) 12, and (e, f) 24 h.

$Cu(CH_3COO)_2 \cdot H_2O$, respectively. Figure 6a shows SEM image of CuO/Cu_2O composite hollow microspheres obtained in a 0.02 M $Cu(CH_3COO)_2 \cdot H_2O$ aqueous solution at 200 °C for 12 h. Compared with the samples obtained at a higher concentration (0.1 M), the diameter of the composite hollow microspheres obtained at a lower concentration shows an obvious decrease from ca. 2 μm to ca. 500 nm. TEM image (Figure 6b) clearly indicates that these composite microspheres exhibit an obvious hollow structure. With increasing reaction concentration of $Cu(CH_3COO)_2 \cdot H_2O$, the diameter of CuO/Cu_2O composite hollow microspheres has an obvious increase. Figure 7 shows SEM images of the composite hollow microspheres obtained in a 0.2 M $Cu(CH_3COO)_2 \cdot H_2O$ aqueous solution at 200 °C for various time. After reaction for 5 h, the diameter of the microspheres (Figure 7a) is in the range of 2.5−5 μm. Moreover, a small interior pore can be seen in the formed composite hollow microspheres (Figure 7b), indicating that the hollow structures begin to form from the interior of aggregated particles because of the higher unstability of the interior. Compared with the sample obtained in a 0.1 M $Cu(CH_3COO)_2 \cdot H_2O$ solution, a higher precursor concentration (0.2 M) is more suitable for a rapider core evacuation. With increasing the reaction time from 5 to 12 h, the shells of the aggregated

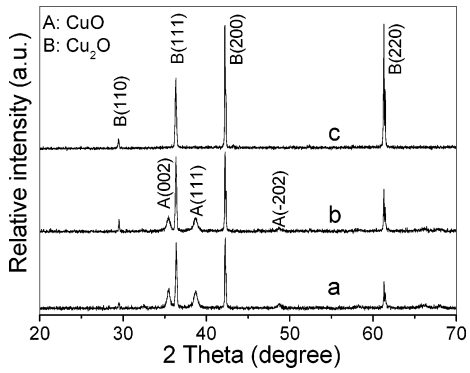

Figure 8. XRD patterns of CuO/Cu_2O composite hollow microspheres obtained in a 0.2 M $Cu(CH_3COO)_2 \cdot H_2O$ aqueous solution at 200 °C for (a) 5, (b) 12, and (c) 24 h.

spherical particles become thinner, as shown in images c and d of Figure 7, respectively. This further confirms that the CuO/Cu_2O composite hollow microspheres are produced by a redistribution of CuO from the interior to the exterior of the microspheres during the hydrothermal treatment. XRD results (Table 1 and Figure 8) indicate that 74.5 and 80.6 wt % Cu_2O existed in the composite hollow microspheres obtained in a 0. 2 M $Cu(CH_3COO)_2 \cdot H_2O$ aqueous solution at 200 °C for 5 and 12 h, respectively. For the composite

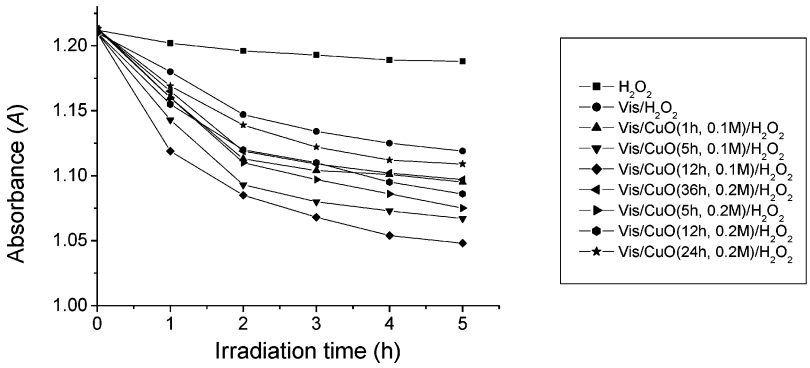

Figure 9. Plots of absorbance (*A*) vs irradiation time (*t*) for the CuO/Cu_2O composite hollow microspheres, the weight of catalysts used for each experiment was 0.2 g. Absorbance (*A*) on the *y*-axis is proportional to the concentration (*c*); "vis" represents visible light.

hollow microspheres obtained from a 0.1 M $Cu(CH_3COO)_2 \cdot H_2O$ aqueous solution at 200 °C for 5, 12, and 36 h, the contents of Cu_2O are 20.1, 23.4, and 68.2 wt %, respectively. Obviously, according to the above results, the contents of Cu_2O in the composite hollow microspheres increase with increasing precursor concentration (see Table 1). Therefore, it can be inferred that a higher CH_3COOH concentration in the reaction solution could accelerate the phase transformation of CuO to Cu_2O. Moreover, the CuO/Cu_2O composite hollow microspheres with a controlled content of 23.4−80.6 wt % Cu_2O can be easily obtained by adjusting the precursor concentration of $Cu(CH_3COO)_2 \cdot H_2O$ or/and reaction time. However, with further increase in the hydrothermal time to 24 h for the 0.2 M $Cu(CH_3COO)_2 \cdot H_2O$ aqueous solution, it was found that only Cu_2O single crystals are obtained and most of them appear to have cubic morphology (images e and f in Figure 7). XRD result indicates that no CuO phase was found in the cubic products (Figure 8c). The formation of Cu_2O single crystals may be due to the existence of more CH_3COOH as a reducing agent of CuO in the solution, resulting in the destruction and restructure of the hollow microspheres and the formation of cubic Cu_2O.

The photocatalytic activity of the samples was evaluated by photocatalytic decolorization of methyl orange aqueous solution in the presence of H_2O_2. Figure 9 shows the comparison of photocatalytic activities of the CuO, Cu_2O, and CuO/Cu_2O composite hollow spheres. It should be noted that in the absence of H_2O_2, the prepared CuO, Cu_2O, and CuO/Cu_2O composite hollow spheres show no photocatalytic activity under visible-light irradiation (not shown here). H_2O_2 alone shows a very weak activity for the decolorization of methyl orange aqueous solution (see Figure 9), whereas in the presence of H_2O_2 and visible-light illumination, methyl orange aqueous solution can be obviously decolorized, probably because of the photodecomposition of H_2O_2 to form a certain amount of $OH^{\bullet}$. It can be seen from Figure 9 that when the CuO (0.1 M, 1 h) or Cu_2O (0.2 M, 24 h) is combined with H_2O_2 and visible light, the concentration of methyl orange shows a faster decrease. This confirms that CuO and Cu_2O can promote the photocatalytic degradation of methyl orange in the presence of H_2O_2 under visible-light illumination. However, when the CuO/Cu_2O composite samples (0.1 M, 12 h) are used as photocatalysts, the concentration of methyl orange shows the fastest decrease, suggesting the highest degradation rate. Therefore, it can be deduced that the composite of CuO and Cu_2O may be beneficial in reducing the recombination of photogenerated electrons and holes and thus enhances photocatalytic activity. This is similar to the heterojunction effect between anatase and rutile two phases in P25 powders with a high photocatalytic activity.[30] The interface between the CuO and Cu_2O might act as a rapid separation site for the photogenerated electrons and holes because of the difference in the energy levels of their conduction bands and valence bands.[31] Therefore, it is not surprised that the pure CuO sample (0.1 M, 1 h) with a higher S_{BER} (45.5 m^2/g) shows a lower degradation rate than the composite sample (0.1 M, 12 h) with a lower S_{BER} (17.7 m^2/g). Of course, the specific surface areas of the composite samples also play an important role in the decolorization of methyl orange aqueous solution, and low S_{BET} would result in a decrease in the photocatalytic activity (Figure 9 and Table 1). However, the exact degradation mechanism of methyl orange in the present system (visible light + CuO/CuO_2 + H_2O_2) still could not be well-understood and further studies would need to be carried out.

4. Conclusion

CuO/Cu_2O composite hollow microspheres could be easily prepared by a simple hydrothermal method using $Cu(CH_3COO)_2 \cdot H_2O$ as precursors. With increasing precursor concentration from 0.02 to 0.2 M, the diameter of hollow composite microspheres increased from 500 nm to 5 μm. Moreover, the content of Cu_2O in composite hollow microspheres increased with increasing reaction time and precursor concentration. The composite hollow microspheres with controllable composition could be prepared by adjusting the reaction time and precursor concentration. A higher precursor concentration was suitable for more rapid core evacuation and phase transformation of CuO to Cu_2O. Compared with the single-phase CuO or Cu_2O samples, the prepared CuO/Cu_2O composite hollow spheres exhibited a higher photocatalytic activity for the photocatalytic degradation of methyl orange aqueous solution under the visible-light illumination

(30) a) Hurum, D. C.; Agrios, A. G.; Gray, K. A.; Rajh, T.; Thurnauer, M. C. *J. Phys. Chem. B* **2003**, *107*, 4545.)b) Yu, J.; Yu, J. C.; Leung, M. K. P.; Ho, W.; Cheng, B.; Zhao, X.; Zhao, J. *J. Catal*. **2003**, *217*, 69. (c)Yu, J.; Yu, H.; Cheng, B.; Zhao, X.; Yu, J. C.; Ho, W. *J. Phys. Chem. B* **2003**, *107*, 13871.

(31) Yu, J.; Zhang, L.; Cheng, B.; Su, Y. *J. Phys. Chem. C* **2007**, *111*, 10582.

in the presence of H_2O_2. Considering the unique hollow structures and their controllable composite, the obtained CuO/Cu_2O composite hollow microspheres might find various potential applications in catalysis, electronics, and optics.

Acknowledgment. This work was partially supported by the National Natural Science Foundation of China (20473059 and 50625208). This work was also financially supported by the Key Research Project of Chinese Ministry of Education (106114) and the Program for Changjiang Scholars and Innovative Research Team in University (PCSIRT, IRT0547), Ministry of Education, China.

CM070386D